



ELSEVIER

Diamond and Related Materials 6 (1997) 1135–1142

**DIAMOND
AND
RELATED
MATERIALS**

Field-emission studies of boron-doped CVD diamond films following surface treatments²

N.A. Fox^{a,*}, S. Mary^{a,1}, T.J. Davis^a, W.N. Wang^a, P.W. May^a, A. Bewick^a,
J.W. Steeds^a, J.E. Butler^b

^a *Diamond Group, University of Bristol, Bristol, UK*

^b *Naval Research Laboratory, Washington, USA*

Received 10 September 1996 accepted 11 February 1997

Abstract

The electron emission from highly twinned, undoped Chemical Vapour Deposited (CVD) diamond thin films has been found to exhibit a stable voltage threshold of $15 \text{ V } \mu\text{m}^{-1}$. In this study the same material has been boron-doped by ion-implantation at two different energy profiles. A number of surface treatments including, Excimer laser annealing, hydrogen passivation, argon/oxygen plasma etching and also coating with gold, were employed in an attempt to enhance the electron emission properties of the highly twinned surface. It has been found that these treatments tend to degrade the electron emission performance, promoting more surface damage and instability in the electron emission current. These results are compared against the emission performance of samples of high quality boron-doped material exhibiting both similar and dissimilar surface textures. © 1997 Elsevier Science S.A.

Keywords: Field-emission; CVD diamond; Boron doping; Surface treatment

1. Introduction

The successful application of diamond as a cold cathode material in vacuum microelectronic devices, such as the Field-emission Display (FED), requires electrodes that exhibit a low threshold voltage for electron emission ($<1 \text{ V } \mu\text{m}^{-1}$). This property has to be linked to a high density of active emission sites ($\sim 10^6 \text{ mm}^{-2}$) being evenly distributed over a given pixel-sized area of the cathode surface. This latter requirement needs to be satisfied without having to rely upon extensive voltage conditioning of the electrode surface area. A number of reports [1] have made reference to the significant changes in surface structure that take place due to dielectric breakdown occurring within the diamond film during emission tests. The primary focus of the work reported here was to determine whether post-growth surface treatment could offer a way to stabilise

the highly twinned diamond film against dielectric breakdown. This type of diamond film contains a high density of sub- μm wedge structures which emit electrons from their sharp edge features (Fig. 1).

Field-emission has been observed from natural type IIb single crystals[2] and from CVD-produced films that have been doped with boron[3]. The means by which field-emission is produced by p-type diamond is still not fully understood but the material has been studied by STM-CITS[4] and by UPS[5].

On hydrogen-terminated material, a Negative Electron Affinity (NEA) has been detected on (111)[5] and (001)[6] crystal facets. On lightly doped single crystal material photo-emission studies have revealed that the source of field-emission is electrons that originate from the valence band[7].

The source of field-electron emission from p-type CVD diamond films is further complicated by the existence of a high density of grain boundaries. The inter-grain regions of these polycrystalline films tend to contain localised concentrations of non-diamond carbon which exhibit different conduction properties compared to the boron-doped polycrystals. The presence of graphitic forms of carbon is known to quench the NEA at

* Corresponding author. Permanent address: Smiths Industries Aerospace, Corporate Research Department, Building CH15, Bishopscleeve, UK.

¹ Permanent address: University of Bordeaux, France.

² Presented at the DIAMOND 1996 Conference, 8–13 September, 1996, Tours, France.

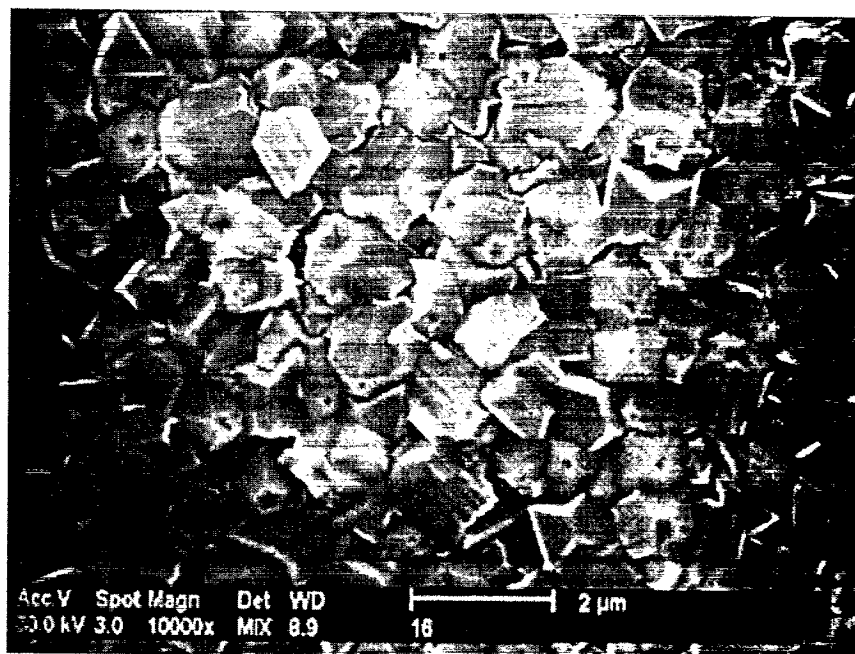


Fig. 1. SEM photograph of the highly twinned material, TW3 and TW4, exhibiting the characteristic pentagonal wedge structures.

a crystal surface[8] and cause the depletion of boron at grain boundaries[9].

The highly twinned films studied here are deemed to contain non-diamond carbon localised principally in the interfacial layer that links the diamond film to the silicon substrate. It is not known whether the presence of this material is disadvantageous to the electron emission performance of the diamond film or if it influences the onset of dielectric breakdown. By employing surface treatments to alter the electron emission of the diamond surface some conclusions may be drawn about the suitability of this material as a field electron emitter.

2. Experimental details

Sample boron-doped diamond films were prepared in accordance with the schedule given in Table 1. A twinned

film growth was exhibited by the free-standing material, identified as NRL5K80, produced by boron incorporation during growth, and by the silicon-supported material that was ion-implanted with boron after CVD growth. The latter material exhibits the higher density of twinned crystals. In Table 1 this material is identified as samples TW3, TW4, and that this film was grown with a high methane fraction producing the film structure illustrated in Fig. 1. The highly twinned material exhibited a Raman profile shown in Fig. 2. The third material identified as New2, is a high quality, free-standing material, containing very few twinned crystals, and contains boron that was ion-implanted after CVD growth.

The schedule of ion-implantation experiments is detailed in Table 2. All of the implantation experiments were performed at liquid nitrogen temperature to try to

Table 1
Schedule of CVD growth

Sample no., (Growth method)	Nucleation conditions ^a	Growth conditions	Post-growth
TW3, (MPCVD) {grown on p(100) Si}	$f=4\%$; $T=925\text{ }^{\circ}\text{C}$; $B=-170\text{ V}$; $P=85\text{ torr}$; $E=2800\text{ W}$; $t=15\text{ min}$.	$f=12\%$; $T=925\text{ }^{\circ}\text{C}$; $B=0\text{ V}$; $P=65\text{ torr}$; $E=2500\text{ W}$; $t=4\text{ h }45\text{ min}$	H_2 plasma: $f=0\%$; $T=925\text{ }^{\circ}\text{C}$; $B=0\text{ V}$; $P=65\text{ torr}$; $E=2500\text{ W}$; $t=10\text{ min}$.
TW4, (MPCVD) {grown on n(111) Si}	$f=4\%$; $T=950\text{ }^{\circ}\text{C}$; $B=-170\text{ V}$; $P=85\text{ torr}$; $E=2800\text{ W}$; $t=15\text{ min}$.	$f=12\%$; $T=925\text{ }^{\circ}\text{C}$; $B=0\text{ V}$; $P=65\text{ torr}$; $E=2500\text{ W}$; $t=4\text{ h }45\text{ min}$	H_2 plasma: $f=0\%$; $T=925\text{ }^{\circ}\text{C}$; $B=0\text{ V}$; $P=65\text{ torr}$; $E=2500\text{ W}$; $t=10\text{ min}$.
NEW2, (MPJCVD) {grown on intrinsic (100) Si}	$f=1\%$; $T=900\text{ }^{\circ}\text{C}$; $B=0\text{ V}$; $P=30\text{ torr}$; $E=5\text{ kW}$; $t=15\text{ min}$.	$f=4\%$; $T=900\text{ }^{\circ}\text{C}$; $B=0\text{ V}$; $P=30\text{ torr}$; $E=5\text{ kW}$; $t=3\text{ h}$.	H_2 plasma: $f=0\%$; $T=925\text{ }^{\circ}\text{C}$; $B=0\text{ V}$; $P=30\text{ torr}$; $E=5\text{ kW}$; $t=10\text{ min}$
NRL 5K80, (MPCVD) {grown on intrinsic (100) Si}	$f=0.5\%$; $T=950\text{ }^{\circ}\text{C}$; $B=0\text{ V}$; $P=25\text{ torr}$; $E=2.5\text{ kW}$; $t=12\text{ h}$	$f=2\%$; $T=850\text{ }^{\circ}\text{C}$; $B=0\text{ V}$; $P=25\text{ torr}$; $E=2.5\text{ kW}$; $t=12\text{ h}$	H_2 plasma: $f=0\%$; $T=925\text{ }^{\circ}\text{C}$; $B=0\text{ V}$; $P=25\text{ torr}$; $E=2.5\text{ kW}$; $t=10\text{ min}$

^aWhere f denotes methane fraction in hydrogen, T denotes substrate temperature, B denotes substrate bias, P denotes working pressure, E denotes microwave power level and t denotes process time.

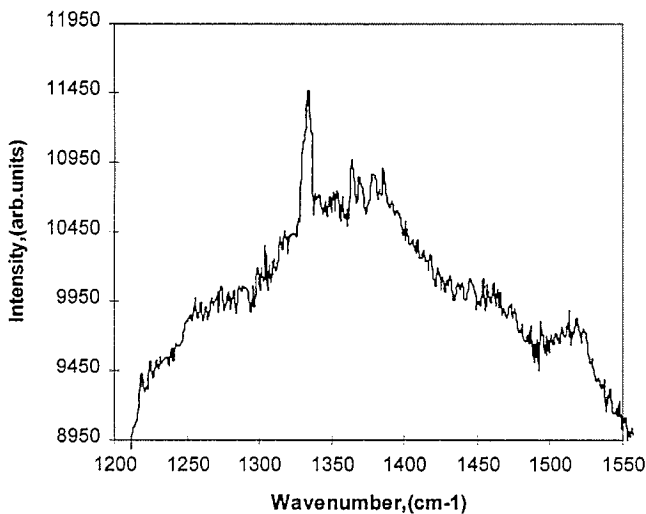


Fig. 2. Raman spectrum of TW3 prior to treatment.

minimise the ion damage to the diamond film samples. Two different implantation profiles were employed to produce doped material in which the implanted species resided at different depths in the film. Doping was achieved by incorporating boron atoms using $^{10}\text{B}_2^+$ and $^{11}\text{B}_2^+$ sources. It should be noted that $^{10}\text{B}_2^+$ was employed for implanting New2 to achieve a near surface dopant layer. This enabled a reduced beam current to be used to obtain the single low-energy dose.

For the case where Rapid Thermal Annealing was employed following implantation, the sample was processed in a vacuum furnace containing a forming gas atmosphere. Initially the sample was heated slowly to 500 °C in a cooler zone of the furnace, to drive off water vapour. Then it was moved into a 1000 °C zone for 10 min, after which it was moved to cool down in the inert gas flow.

Laser annealing was undertaken at an Excimer laser wavelength of 193 nm using a Lambda Physik Compex

system, which delivered an average fluence of 100 mJ cm⁻² to the sample film per pulse. A pulse repetition rate of 1 Hz was used in this study to irradiate a given sample for periods of 50, 100 and 200 s.

An RF plasma etch using an 80% argon:20% oxygen gas mixture was used to etch the implanted sample films in an attempt to reveal a fresh surface containing dopant atoms which could then be hydrogen passivated. During the RF etch treatment, the sample films were exposed to a power level of 200 W at a base pressure of 30 torr for 30 min; the temperature of the sample did not exceed 60 °C during exposure.

Hydrogen plasma treatment of the films was performed in a MPCVD reactor at a power level of 1 kW, at 30 torr and with the substrate maintained at a temperature of 500 °C. Based upon an earlier study that recorded the change in field-electron emission with plasma exposure, using undoped CVD diamond, the exposure time adopted was 25 min.

Surface analysis was carried out using a Renishaw 2000 Ramanscope system, and a JEOL 6400 Scanning Electron Microscope (SEM).

The field-emission studies were conducted using a dedicated vacuum pumping station, that could achieve a base pressure of 2×10^{-7} torr, and which was linked to a glass diode test cell. Current–voltage measurements were recorded using a 3 mm (o.d.) copper rod anode. Images of the electron emission could be generated by replacing the copper anode with an ITO screen spaced away from the diamond film by glass fibre spacers. A CCD camera was used in combination with a PC-based video capture card to acquire pictures of the emission sites. Current–voltage and stability measurements were recorded using a menu-driven program written in Qbasic. The control software performs voltage ramping cycles over a chosen range and then stores the current, voltage data to disk. A second Qbasic program was

Table 2
Schedule of ion-implantation

Sample	Ion species	Nucleon energy (keV)	Dose ($\times 10^{13}\text{cm}^{-2}$)	Anneal	Maximum concentration ($\times 10^{18}\text{cm}^{-3}$)
TW3	$^{11}\text{BF}_2^+$	50	0.158	No RTA	50 (flat profile)
		40	0.635		
		30	0.122		
		20	0.105		
TW4/1	$^{11}\text{BF}_2^+$	2000	0.73	RTA	10 (flat profile)
		1900	0.745		
		1800	0.813		
		1700	0.819		
TW4/2	$^{11}\text{BF}_2^+$	2000	0.73	No RTA	10 (flat profile)
		1900	0.745		
		1800	0.813		
		1700	0.819		
NEW2	$^{10}\text{BF}_2^+$	18.75	10.5	No RTA	45.52
NRL 5K80	—	—	—	—	—

Table 3
Voltage thresholds for field-emission recorded with a 20- μm anode-cathode gap

Sample	Untreated	After laser anneal + H_2 passivation	After Ar/ O_2 etch + H_2 passivation	After coating with gold
TW3	$10 \text{ V } \mu\text{m}^{-1}$	$20 \text{ V } \mu\text{m}^{-1}$	destroyed	$14 \text{ V } \mu\text{m}^{-1}$
New2	$46 \text{ V } \mu\text{m}^{-1}$	$22 \text{ V } \mu\text{m}^{-1}$	$17 \text{ V } \mu\text{m}^{-1}$	not treated
TW4/1	$22 \text{ V } \mu\text{m}^{-1}$	not treated	destroyed	$39 \text{ V } \mu\text{m}^{-1}$
TW4/2	$13 \text{ V } \mu\text{m}^{-1}$	$23 \text{ V } \mu\text{m}^{-1}$	destroyed	$48 \text{ V } \mu\text{m}^{-1}$
NRL 5K80	$16 \text{ V } \mu\text{m}^{-1}$	not treated	$36 \text{ V } \mu\text{m}^{-1}$	$40 \text{ V } \mu\text{m}^{-1}$

then used to process the experimental data to compute the threshold voltages and currents and to plot I–V and Fowler–Nordheim graphs.

Voltage-current data recorded prior to surface treatment with an anode-cathode gap of 20 microns.

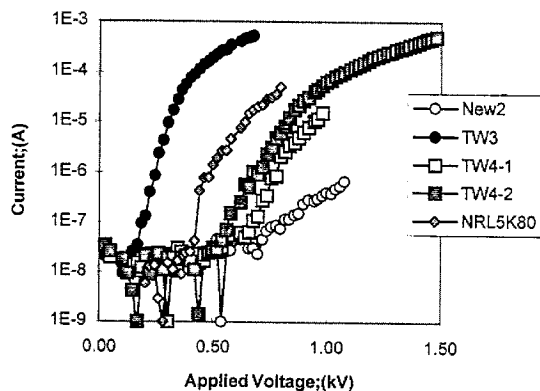


Fig. 3. Electron emission from the untreated films showing that the lowest voltage threshold is exhibited by the highly twinned, low energy boron-implanted film, TW3.

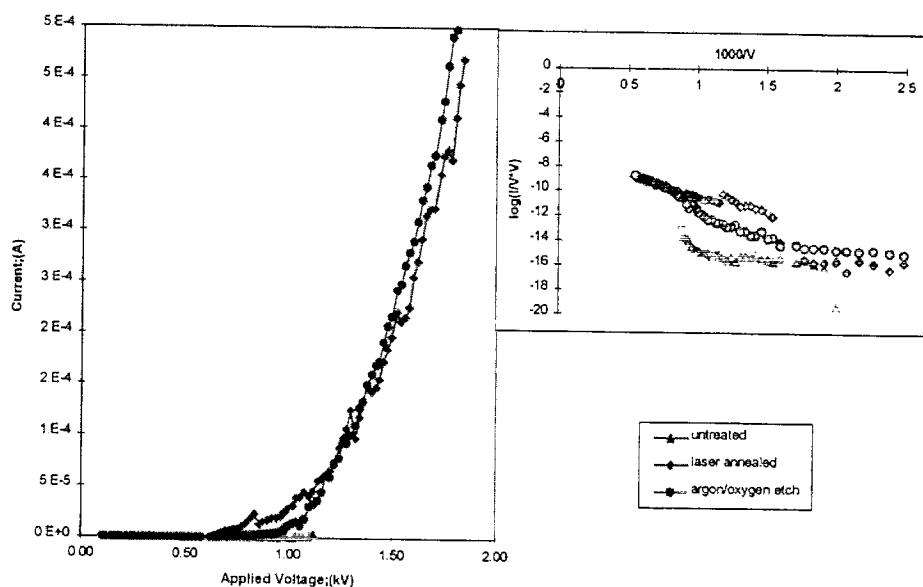


Fig. 4. Field-emission plots for different treatments performed on sample New2.

3. Experimental results

3.1. The effect of surface treatment upon field-emission threshold

The threshold fields given in Table 3 are the values obtained for an applied voltage ramp up and are the average values obtained from three different test areas on a given sample film. Surface treatment was found to degrade the emission performance of the highly twinned material and to show significantly more structural damage to the surface region. The data listed for the laser annealing treatment was obtained with the 100 s exposure level which gave the least degradation in threshold for TW3 and TW4. Under the same conditions New2 recorded a significant reduction in switch-on threshold and an enhanced emission current, rising from 4×10^{-6} to 500×10^{-6} A at $70 \text{ V } \mu\text{m}$. The highly twinned material was almost completely consumed during the argon plasma treatment while the reference samples showed little physical change. Fig. 3 gives typical current–voltage characteristics for the untreated films. Fig. 4 presents data on New2 following successive surface treatments. Fig. 5

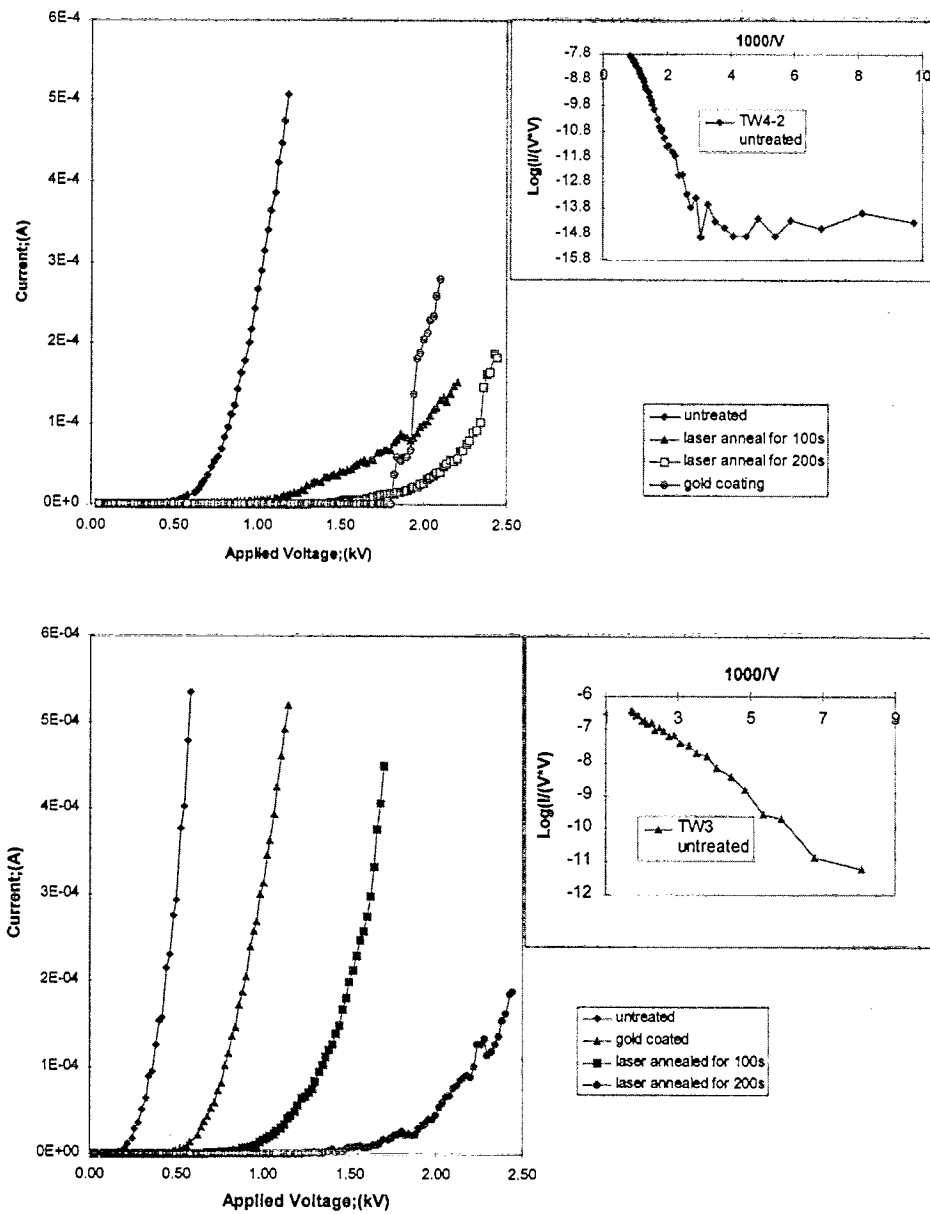


Fig. 5. Field-emission plots for different treatments performed on TW3 and TW4.

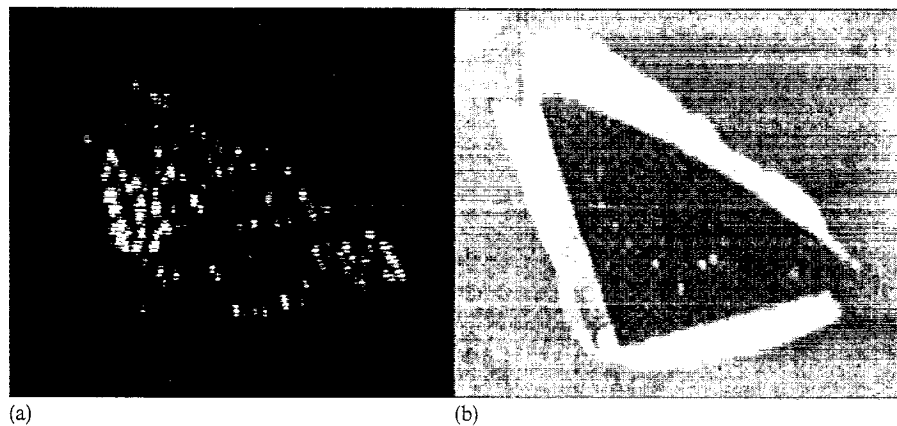


Fig. 6. Image of FE sites on TW3 sample viewed with: (a) room lighting off; (b) room lighting on.

presents data obtained for the highly twinned samples following surface treatment. The distribution of emission sites that can be achieved with TW3 material is illustrated in Fig. 6. These images were taken at 1850 V using a diode configuration with a 50- μm gap. The sample is about 0.3 cm^2 and the integral emission current was 0.65 mA. The resolution of these CCD images was not sufficient to allow a determination, by image processing techniques, of the number of active emission sites. However the distribution of emitters contributing to the integral emission current was very uniform.

3.2. *The effect of surface treatment upon the Raman diamond line-width*

It has been suggested that the field-emission behaviour of a given diamond film may be inferred from its characteristic linewidth [10]. The most promising surface treatment in terms of its ability to modify the linewidth was the Excimer laser irradiation which facilitated a reduction in the 1332 cm^{-1} linewidth for the highly twinned material as well as for New2. However it should be noted that all of the surface treatments on TW3 produced a narrower linewidth than the untreated material. The half width half maximum values given in Table 4 should be compared against the measured half-width half maximum value obtained for a natural (IIa) diamond of 2.08 cm^{-1} at 1332.3 cm^{-1} . The peak position for the diamond line measured for each material is detailed in the table in brackets.

3.3. *Analysis of emission sites following field-emission measurements*

It has been previously reported that CVD films are prone to dielectric breakdown and that this results in irreversible changes to the surface texture. The initial current-voltage "hysteresis" exhibited by some films can be attributed to this surface disruption. For the twinned CVD films measured here it has been found that rather than the electron emission causing cratering, grain sized "blind" holes, 1–2 μm in diameter were punched into the film. This was found to occur for field-strengths above $60\text{ V }\mu\text{m}^{-1}$. No evidence of surface damage could be detected on sample New2, but the surface of the

NRL sample did show some localised changes. Most notable was the appearance of clusters of particles on crystal facets that had been situated within the zone of influence ($\sim 100\text{ }\mu\text{m}$) of an area tested for field-emission. Fig. 7(a) shows a region of the sample that contains an emission site. In Figs. 7(b) and 7(c) the particles that appear on crystal facets in the emission site region are clearly seen.

4. Conclusions

In general it was found that the laser annealing surface treatment was effective at reducing the defects present within a given CVD film.

However, in the case of the twinned diamond films, this improvement in diamond quality was gained at the expense of an increase in the applied electric field required to initiate electron emission.

By comparing the electron emission performance of TW4/1, the RTA sample, with TW4/2 which had been laser annealed, it can be concluded that the laser annealing at 193 nm has a similar effect upon the diamond film surface as the RTA treatment. This suggests that the defects introduced by the ion-implantation process have not been completely removed by the laser annealing of TW3. These observations would suggest that the amount of non-diamond material included in the highly twinned film during growth needs to be more carefully controlled.

The Raman studies show that the high quality, free-standing sample New2, responds better to post-implantation annealing than the lower quality TW3 material. New2 is irradiated with a lower implantation energy, but owing to the dopant concentration being about the same as TW3, this difference could not be attributed to the implantation profiles.

In the case of New2, it would appear that initially field-emission is being induced from a sub-surface region. Following laser annealing, the defect density due to the implantation damage is observed to be reduced. Contact measurements show the surface conductivity of the sample to be significantly improved compared to the untreated material. Therefore, it would appear that the improvement in the electron emission can be attributed

Table 4
Raman "diamond" linewidths for the sample films

	Untreated	After laser anneal	After laser anneal + H_2 passivation	After coating with gold
TW3	3.66 cm^{-1} (1332.7)	2.70 cm^{-1} (1333.5)	3.35 cm^{-1} (1333.3)	3.55 cm^{-1} (1332.8)
TW4/1	4.18 cm^{-1} (1333.3)	Not treated	Not measured	Could not be fitted
TW4/2	3.94 cm^{-1} (1330.3)	2.03 cm^{-1} (1332.2)	Not measured	5.49 cm^{-1} (1332.2)
New2	3.99 cm^{-1} (1332.2)	2.19 cm^{-1} (1332.7)	Not measured	Not treated
NRL 5K80	2.05 cm^{-1} (1332.2)	Not treated	Not measured	2.03 cm^{-1} (1332.2)

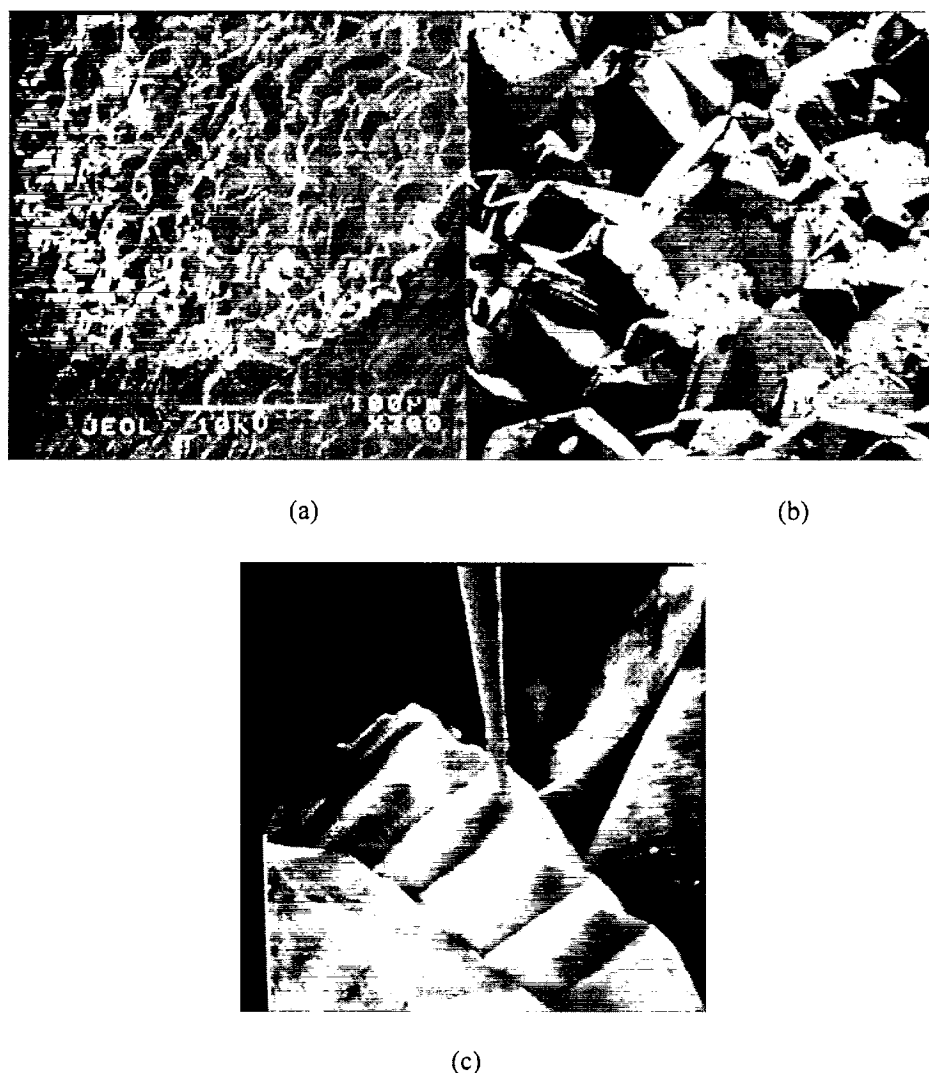


Fig. 7. SEM pictures of NRL5K80 showing: (a) regions of high and low secondary electron emission; (b) 1 kV, $\times 1000$ image of facets in a field-emission site; (c) 17.5 kV, $\times 5000$ image of the particles that dress the facets in a field-emission site.

to the efficient activation of the implanted impurities. The further enhancement in emission threshold following the argon/oxygen etch, suggests that the new surface is closer to the impurity level in the film allowing more efficient ejection of electrons into the vacuum.

The New2 material is also found to be less susceptible to dielectric breakdown effects than the other CVD samples.

The NRL 5K80 sample exhibited a degradation in electron emission performance which upon inspection seemed to be associated with the appearance of particles on crystal grains that resided within the general area from which field-emission was recorded. Considering the high quality of this sample film it has not been possible to ascertain the mechanism by which this degradation occurs.

Acknowledgement

This work was supported by EPSRC ROPA grant No.GRK65133. Neil Fox is an Industrial Fellow of the Royal Commission for the Exhibition of 1851, London and would like to thank Smiths Industries Aerospace for their support of this work. The authors are grateful to Professor G. Allen (Interface Analysis Centre, University of Bristol) for making available the Raman system, and to Professor Mike Ashfold (Chemistry) for the use of the Excimer laser system. Ion-implantation work was conducted at the University of Surrey. The construction of experimental equipment by the Physics Department's Workshop staff, John Rowden and Ken Dunn, along with the technical support given by Jerry Hart, and George Shaw, is also gratefully acknowledged.

References

- [1] L.S. Pan, Material Research Society Symposium Proceedings, Fall meeting, Boston, 1995, vol. 416, p. 407.
- [2] M. Geis, N.N. Efremow, J.D. Woodhouse, M.D. McAleese, M. Marhywka, D.G. Socker, J.F. Hochedez, *IEEE Devel. Lett.* 12 (8) (1991) 456.
- [3] D. Hong, M. Aslam, *J. Vac. Sci. Technol. B.* 13 (2) (1995) 427.
- [4] W.N. Wang, N.A. Fox, J.W. Steeds, J.E. Butler, *J. Appl. Phys.* 80 (1996) 407.
- [5] B.B. Pate, *Surf. Sci.* 165 (1986) 83.
- [6] P.K. Baumann, R.J. Nemanich, *Diamond Relat. Mater.* 4 (1995) 802.
- [7] C. Bandis, B.B. Pate, *Appl. Phys. Lett.* 69 (1996) 3.
- [8] F.J. Himpsel, D.E. Eastman, J.F. van der Veen, *J. Vac. Sci. Technol.* 15 (5) (1980) 1085.
- [9] J.T. Huang, C.S. Hua, J. Hwang, H. Chang, L.J. Lee, *Appl. Phys. Lett.* 67 (16) (1995) 2382.
- [10] W. Zhu, *J. Appl. Phys.* 78 (10) (1995) 2707.